J. Fluid Mech. (1965), *vol.* 22, *part* 1, *pp.* 135–159
Printed in Great Britain

The uniform distortion of a turbulent wake

By J. F. KEFFER
Cavendish Laboratory, Cambridge*

(Received 14 August 1964)

The effect of a uniform and constant rate of strain imposed upon a turbulent wake which is generated behind a circular cylinder has been examined experimentally. The strain field, produced by passing the flow through a distorting duct of constant cross-sectional area, simultaneously compresses the wake in the plane of the cylinder and extends it in the other lateral direction but applies no strain in the direction of the main stream. The investigation shows the existence of a large-scale, periodic eddy structure within the strained wake, similar to, but more intense than, that which was observed for the undistorted wake. These large lateral convective motions appear to be the primary mechanism controlling the development of the flow, and are responsible for the failure of the wake to attain the theoretically predicted self-preservation state. It is shown that the strain rate, which acts favourably upon these large eddies, is sufficient to produce a net increase in vorticity in spite of the ordinary processes of turbulent viscous decay. At the same time, however, the rate of viscous dissipation of the smallest eddies in the flow is augmented by the strain, and the resulting wake structure is almost entirely dominated by the large-eddy motions. A possible means by which the large eddies are initiated is discussed.

1. Introduction

The sudden straining of a turbulent flow first became of interest in the design and construction of early wind tunnels and more recently in the development of modern low-turbulence tunnels. It was found that a contraction, placed just upstream of the working section of the tunnel, reduced the ratio of the mean turbulent kinetic energy relative to the energy of the main stream. There was, however, a simultaneous increase in the anisotropy of the individual components of the turbulent intensities. Prandtl (1933) was able to explain the observed anisotropy of the lateral components, qualitatively, by an argument based upon the stretching and contracting of inviscid vortex filaments which were aligned in different directions to the main stream. The analysis was extended by Taylor (1935), who described the action of a wind-tunnel contraction upon a single Fourier component, i.e. a cellular vortex which could be considered a single periodic motion in three dimensions. A more general treatment by Ribner & Tucker (1952) and Batchelor & Proudman (1954) treated all Fourier components, assuming that the strain was applied homogeneously and sufficiently rapidly so that no appreciable viscous decay or inertial interaction took place. The former

* Now at the Department of Mechanical Engineering, University of Toronto, Canada.

requirement is not unrealistic for most wind tunnels, but the latter condition cannot be expected to be met in a real flow. Their results predicted well the total change in turbulent kinetic energy, but less successfully the magnitude of the observed anisotropy.

The effect of a constant and uniform strain rate upon a homogeneous turbulence was first investigated by Townsend (1954). The results agreed qualitatively with the first-order theory of Ribner & Tucker, and Batchelor & Proudman, for a rapid strain, in showing the expected redistribution of turbulent energy along the principal axes of strain. The rate of strain was not large enough, however, to prevent viscous and inertial transfer terms in the equations of motion from becoming significant. Nevertheless, it was possible to reconcile the behaviour of the flow for small total strains with the first-order theory by including the effects of the viscous decay.

It was of some interest to look at the effect of an applied rate of strain to the structure of a more complicated flow, and the first experimental investigation of a free turbulent shear flow was made by Reynolds (1962), who examined the two-dimensional wake which was compressed laterally in the plane of the cylinder and simultaneously expanded in the other lateral direction, i.e. along the cylinder axis. Clearly the analytical arguments mentioned above could not be expected to apply since the presence of a mean-velocity defect complicates the analysis. Reynolds did show that a state of self-preservation was theoretically possible, and his measurements tended to suggest a trend towards this self-preservation for certain conditions of the applied rate of strain. The present measurements appear to preclude this possibility, however.

Previous investigations of the structure of the unstrained wake have made clear the existence of two distinct types of motion. The one, which may be associated with length scales an order of magnitude smaller than the dimensions of the flow system, and which contains most of the turbulent energy of the flow, can be successfully described as a more or less homogeneous group of eddies distributed throughout the turbulent fluid. Townsend's work on the distortion of homogeneous turbulence showed that these motions respond directly to the strain. The implication is that, in a shear flow, the energy-containing eddies are directly affected by the mean strain produced by the velocity gradient and reach a state of equilibrium relatively quickly. It would appear that these eddies have little direct effect upon the gross development of the flow, however. The large-scale process of entrainment is effected by another group of eddies roughly the size of the flow system itself, and acting independently of the small structure. A great deal of attention has been attracted to this aspect of the problem since these eddies are primarily responsible for the lateral growth of a turbulent shear flow. The investigations of Grant (1958) for the unstrained wake have revealed the general structure of the large-scale motions. That these eddies must exist in a type of dynamic equilibrium in such a developing flow is clear, and, although this state must depend upon the past history of the eddy, the details of the growth and decay processes are not at all obvious.

The investigation described in this paper was undertaken with the view of examining the way in which the detailed structure of the turbulent wake reacts

to a constant and uniform strain rate. For moderate total strains, the simpler, homogeneous turbulence responds by achieving a balance between the orientating effect of the distortion and the natural movement of the eddies towards isotropy. One might expect the strained wake to exhibit the same general tendency, at least in the energy-containing eddy range. The strain field within the wake which results from the mean shear, however, introduces an essential difference, since the axes of the two strain fields are not coincident. The response of the large-eddy motions to the strain is also significant, and an attempt is made here to gain a clearer understanding of the way in which they influence the flow generally.

2. Description of the flow

A constant and uniform rate of strain was produced by passing the flow through the distorting duct shown schematically in figure 1. Ox is the direction of the main stream, and Oy and Oz complete the Cartesian co-ordinate system. The

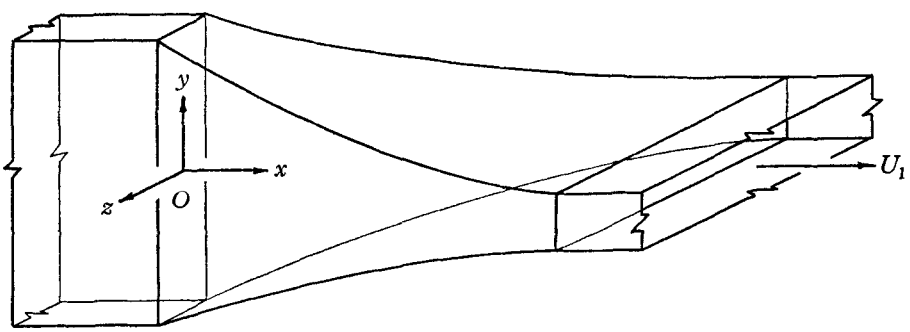

FIGURE 1. Distorting section of wind tunnel.

cross-sectional area remains constant so that no acceleration is applied to the fluid in the stream direction. The exponentially varying sides, described by

$$y = y_0 \exp\{-a(x-x_0)\}, \tag{2.1}$$

$$z = z_0 \exp\{a(x-x_0)\}, \tag{2.2}$$

where the subscript zero refers to conditions at the entrance to the distortion, define the mean stream lines for the convective flow in the duct. The resulting velocity field is

$$U = U_1 = \text{const.}, \tag{2.3}$$

$$V = -ayU_1, \tag{2.4}$$

$$W = azU_1, \tag{2.5}$$

and the rate of strain tensor for this particular geometry is therefore

$$\alpha_{ij} = \partial u_i/\partial x_j = \begin{Bmatrix} 0 & 0 & 0 \\ 0 & -aU_1 & 0 \\ 0 & 0 & aU_1 \end{Bmatrix}, \tag{2.6}$$

satisfying the condition of incompressibility, $\alpha_{ii} = 0$. The undisturbed convection field thus applies a pure strain rate in the two lateral directions only, contracting the flow in the y-direction and simultaneously expanding it in the z-direction.

Measurements within the duct show that the applied strain is homogeneous in the lateral directions except in the boundary layers. Only near the exit of the distortion does the wake width become large enough to be influenced by the walls of the tunnel. The longitudinal mean velocity is constant throughout the duct except near the exit and entrance. The impossibility of commencing instantaneously a constant rate of strain causes slight flow separations at these points, which effectively decrease the cross-sectional area and increase the mean velocity by approximately 6 %. This had no appreciable influence upon the results, however.

A qualitative indication of the expected behaviour of a turbulent field in this convecting flow can be obtained by supposing the turbulence to consist of a finite collection of small inviscid eddies, randomly orientated to the axes of strain. We examine three typical eddies with their vorticity axes aligned with the principal axes of the system.

The total strain ratio γ_i at any position $(x-x_0)$ in the distorting duct is, for the three co-ordinate directions,

$$\gamma_1 = 1,$$
$$\gamma_2 = \beta,$$
$$\gamma_3 = \beta^{-1},$$

where $\beta = \exp\{-a(x-x_0)\}$, and $\gamma_1\gamma_2\gamma_3 = 1$ from continuity. The vorticity of the longitudinal eddy will remain unaffected by the distortion so that the peripheral velocities at some arbitrary radius are

$$v_1 = v_0,$$
$$w_1 = w_0.$$

In the two lateral directions Oy and Oz, the vorticity of the eddies is altered by the strain, and the velocities become

$$u_2 = \beta u_0,$$
$$w_2 = \beta w_0,$$

and

$$u_3 = \beta^{-1}u_0,$$
$$v_3 = \beta^{-1}v_0,$$

respectively. The averaged effect of the strain is to generate an anisotropy, of the components,

$$u = u_0,$$
$$v = \beta^{-1}v_0,$$
$$w = \beta w_0.$$

In a real fluid, the viscous decay of turbulent energy is sufficient to prevent an absolute increase in any single intensity component, at least with strain rates that can usually be generated experimentally. One would expect to find, however, a redistribution of energy along the axes of strain for any turbulent flow subjected to this distortion field.

In the present series of tests, the wake was produced upstream from the distortion, the axis of the cylinder lying perpendicular to the plane $z = 0$, at the

position $y = 0$. The Reynolds number was sufficiently large so that within a few diameters of the cylinder the flow had become fully turbulent, entering the distorting duct in that state. In the absence of a more elaborate treatment, it is necessary to examine the conditions for self-preservation. Following the general method of Reynolds (1962), the analysis is restricted to the plane of symmetry $z = 0$, and it is assumed that any expansion of the wake is small enough for the lateral pressure gradient terms to be ignored.

By introducing the usual boundary-layer simplifications, the full mean equations of motion

$$U_j \frac{\partial U_i}{\partial x_j} + \frac{\partial \overline{u_i u_j}}{\partial x_j} = -\frac{1}{\rho}\frac{\partial P}{\partial x_i} + \nu \frac{\partial^2 U_i}{\partial x_j^2} \tag{2.7}$$

reduce to

$$U_1 \frac{\partial U}{\partial x} - ayU_1 \frac{\partial U}{\partial y} + \frac{\partial \overline{uv}}{\partial y} = \nu \frac{\partial^2 U}{\partial y^2}, \tag{2.8}$$

and

$$a^2 U_1^2 y + \partial \overline{v^2}/\partial y = 0, \tag{2.9}$$

with the equation of continuity

$$\partial U_i/\partial x_i = 0, \tag{2.10}$$

which requires that the mean streamlines of the convecting flow are not significantly affected by the turbulence pattern in the wake. If the rate of strain is not too large, so that

$$a = O(1/l_0),$$

l_0 being a characteristic length scale of the flow system, e.g. the wake width, then the equations of motion are

$$U_1 \frac{\partial U}{\partial x} - ayU_1 \frac{\partial U}{\partial y} + \frac{\partial \overline{uv}}{\partial y} = 0 \tag{2.11}$$

for high Reynolds numbers where viscous effects can be ignored.

A second expression is obtained from the momentum integral equation. This simplifies to

$$\frac{d}{dx}\left\{\beta^{-1}\int_y (U^2 - U_1 U)\, dy\right\} = 0,$$

or

$$\beta^{-1}\int_y (U^2 - U_1 U)\, dy = \text{const.} \tag{2.12}$$

The following self-preservation relationships can now be introduced:

$$\left.\begin{aligned} U &= U_1 + u_0 f(\eta), \\ \overline{uv} &= u_0^2 g_{12}(\eta), \end{aligned}\right\} \tag{2.13}$$

where

$$\eta = y/l_0,$$

and u_0 and l_0 are appropriate velocity and length scales of the flow, say the maximum mean-velocity defect and the half-velocity width, respectively. With these substitutions equation (2.11) becomes

$$\frac{U_1}{u_0}\left[\frac{l_0}{u_0}\frac{du_0}{dx} f(\eta) - \left(\frac{dl_0}{dx} + al_0\right)\eta f'(\eta)\right] + g_{12}'(\eta) = 0, \tag{2.14}$$

and the conditions for self-preservation are simply that the coefficients of the terms are constant, as dictated by the stress term, i.e.

$$\frac{l_0}{u_0^2}\frac{du_0}{dx} = \text{const.}, \tag{2.15}$$

$$a\frac{l_0}{u_0} + \frac{1}{u_0}\frac{dl_0}{dx} = \text{const.} \tag{2.16}$$

The momentum integral (2.12) upon substitution of (2.13) becomes

$$U_1 l_0 u_0 \int_y f(\eta)\,d\eta + u_0^2 l_0 \int_y f(\eta)\,d\eta \propto \beta,$$

and, since $U_1/u_0 \gg |f|$, this reduces to

$$\beta^{-1} u_0 l_0 = \text{const.} \tag{2.17}$$

The final self-preserving forms of the wake scales for this flow then are

$$u_0 \sim \beta^{\frac{1}{2}}, \tag{2.18}$$

$$l_0 \sim \beta^{\frac{1}{2}}. \tag{2.19}$$

For the same restrictions upon the flow, the turbulent-energy equation can be simplified to

$$U_1\frac{\partial(\frac{1}{2}\overline{q^2})}{\partial x} - ayU_1\frac{\partial(\frac{1}{2}\overline{q^2})}{\partial y} + \overline{uv}\frac{\partial U}{\partial y} - (\overline{v^2} - \overline{w^2})\,aU_1 + \frac{\partial}{\partial y}\overline{v\left(\frac{p}{\rho} + \frac{q^2}{2}\right)} + \epsilon = 0. \tag{2.20}$$

If we assume that all turbulence terms depend only upon the velocity scale u_0, the conditions (2.13), together with

$$\begin{aligned}
\tfrac{1}{2}\overline{q^2} &= u_0^2 g_{ii}(\eta), \\
\overline{v^2} &= u_0^2 g_{22}(\eta), \\
\overline{w^2} &= u_0^2 g_{33}(\eta), \\
\overline{v\left(\frac{p}{\rho} + \frac{q^2}{2}\right)} &= u_0^3 h(\eta), \\
\epsilon &= \frac{u_0^3}{l_1} k(\eta),
\end{aligned}$$

where l_1 is a scale characteristic of the eddy size throughout the dissipation range, can be substituted into the turbulent-energy equation (2.20), yielding the self-preserving constraints:

$$\frac{1}{u_0}\frac{dl_0}{dx} = \text{const.}, \tag{2.21}$$

$$\frac{l_0}{u_0^2}\frac{du_0}{dx} = \text{const.}, \tag{2.22}$$

$$al_0/u_0 = \text{const.}, \tag{2.23}$$

$$l_0/l_1 = \text{const.} \tag{2.24}$$

The first three are satisfied by equations (2.18) and (2.19). The last condition corresponds to self-preservation when $l_1 = O(l_0)$, i.e. for all but the smallest eddies

of the flow. The requirement is essentially that the form of the turbulent-energy spectrum should be self-preserving, a rather severe restriction, which is not realized in most turbulent shear flows. Later results show that the shape of the spectrum changes even more markedly in the presence of an external strain field.

3. Experimental investigation

A complete description of the wind tunnel used in the present investigation has been given by Townsend (1954). The length of the distorting section was 40 in. with an entrance 24 by 6 in. changing exponentially to 6·25 by 24·25 in. The increase of cross-sectional area allows for boundary-layer growth. The maximum total-strain ratio was thus $\beta = 4$ at $(x-x_0) = 40$ in. For the main portion of the experiments, the wake was produced with a $\frac{3}{16}$ in. circular cylinder, placed at 110, 53 and 4 diameters upstream from the beginning of the distortion. Wind-tunnel speed was held constant at 18 ft./sec for most tests, giving a Reynolds number based on the cylinder diameter of 1700. A $\frac{1}{2}$ in. and $\frac{5}{16}$ in. cylinder inserted at the furthermost upstream location were used for preliminary investigations.

Where possible, velocity and length scales, $u_0 = (U_1 - U_{\min})/U_1$ and $l_0 = b/d$, respectively, where b is the half-velocity width, were determined by Pitot-tube methods. At large distances from the cylinder it was necessary to define the wake width in terms of the variation of the u-component of turbulent velocity, i.e. $l_0' = b'/d$. A comparison of these methods for the $\frac{3}{16}$ in. cylinder at 4 diameters from the distortion indicated a direct correspondence, the turbulent-wake width being a constant numerical factor, 1·37 times greater than the mean-velocity-defect width.

Measurements of the longitudinal turbulent intensities were obtained with a constant-current hot-wire anemometer. Lateral intensities v', w' and Reynolds stresses were determined by swinging the hot wire through an arc, $\pm 45°$ normal to the mean flow, in the lateral planes $z = 0$ and $y = \text{const.}$

Figure 2 shows the variation of length scale l_0' for cylinders at the furthermost position upstream, i.e. $(x_0 - x_c) = 20$ in., where x_c is the location of the cylinder and x_0 is the beginning of the distortion. The self-preserving form $\beta^{\frac{1}{2}}$, indicated by the above analysis is not attained. It appears, however, that a type of similarity structure develops for total-strain ratios $\beta > 1{\cdot}5$, in that scales of the two smallest cylinders assume a different exponential form from that predicted. The variation of wake width is identically $\beta^{0{\cdot}35}$ in these cases. Since a decrease in cylinder diameter is equivalent to increasing the development length of the wake flow $(x_0 - x_c)/d$ before entering the strain field, the implication is that no closer approach to self-preservation is likely to be achieved by moving the cylinders further upstream.

Figure 3 shows velocity and length scales for the $\frac{3}{16}$ in. diameter cylinder for smaller $(x_0 - x_c)/d$, and again there is no evidence of the predicted self-preservation behaviour. For $(x_0 - x_c) = 10$, l_0 varies as $\beta^{0{\cdot}162}$, whereas, for $(x_0 - x_c) = 0$, the wake width becomes constant for total strains greater than about 2. The effect of the strain upon u_0 is to decrease the mean-velocity defect at a rate greater than

that of the unstrained wake or that predicted by the self-preservation analysis. For $\beta \approx 3{\cdot}5$, i.e. $(x-x_0) = 35$ in., the end effects of the distortion influence the wake as the strain rate is released and the wake width begins to increase.

In all the observed situations the rate of decrease in wake width is less than that required by the theory. It is suggested later in the paper that this arises from an intensification of the motion of the favourably aligned, large eddies, which is fed directly by the strain rate. A stabilization of the turbulence results, allowing a different equilibrium structure to develop.

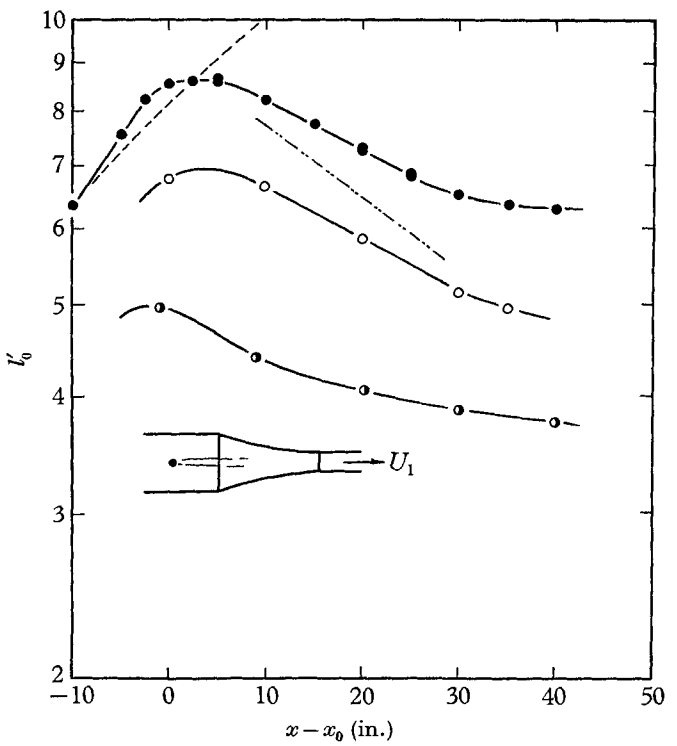

FIGURE 2. Length scales for distorted wake. ●, $\frac{3}{16}$ in. diameter cylinder, $Re_d = 1700$; ○, $\frac{5}{16}$ in., $Re_d = 2800$; ◑, $\frac{1}{2}$ in., $Re_d = 4500$. – – –, unstrained wake (Townsend 1956); —·—·—, $\beta^{\frac{1}{2}}$.

In figure 4, the variation of the turbulent intensities at the wake centre, along the direction of flow, indicates a progressive change in the anisotropy of the components as the total strain increases. The direction of the redistribution of the turbulent energy is in qualitative agreement with the results of the simple, inviscid analysis, v'/U_1 losing energy less rapidly than w'/U_1. The increase in the total turbulent kinetic energy relative to the normal wake is marked, and arises mostly from the additional production term $-(\overline{v^2}-\overline{w^2})aU_1$ in equation (2.20). It is shown later that this extra energy is distributed mainly in the low frequency end of the spectrum, i.e. in the large eddies.

The lateral variation of the turbulence across the wake, plotted in figure 5, shows clearly the anisotropy of the three intensity components. Near the centre

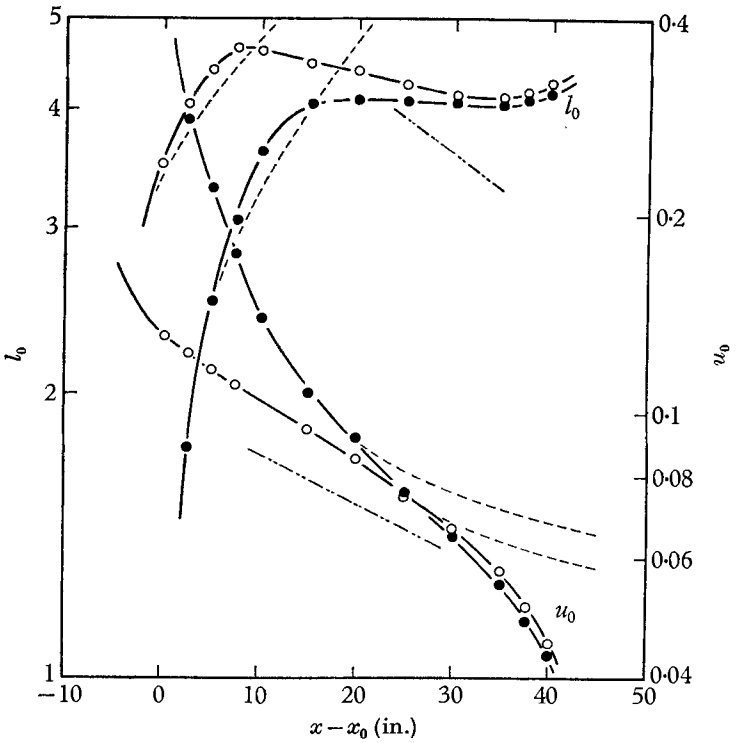

FIGURE 3. Velocity and length scales for strain imposed at different points on the wake. $Re_d = 1700$, $d = \frac{3}{16}$ in. ○, $(x_0-x_c) = 10$ in.; ●, $(x_0-x_c) = 0$ in.; – – –, unstrained wake (Townsend 1956); —·—·—, $\beta^{\frac{1}{2}}$.

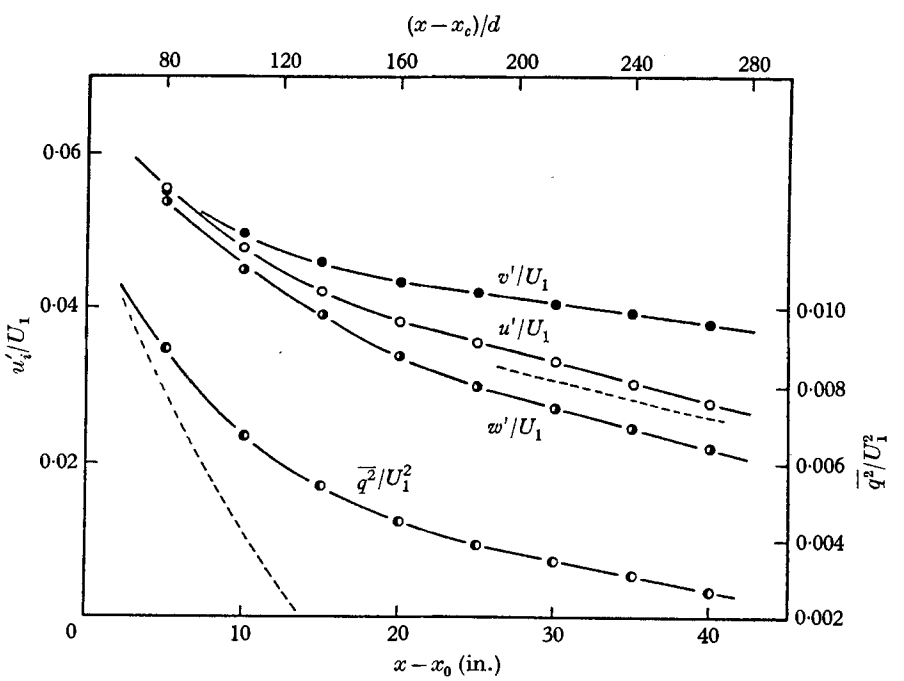

FIGURE 4. Variation of turbulent intensities along the wake axis. $(x_0-x_0) = 10$ in., $Re_d = 1700$, $d = \frac{3}{16}$ in.; – – –, unstrained wake.

of the wake, where u- and w-profiles exhibit a characteristic change of sign in the intensity gradient, the anisotropy is very marked. This decreases towards the edge of the wake as the intensities fall. The Reynolds-shear-stress coefficient, $-\overline{uv}/\overline{u^2}$ is generally similar to that of the unstrained wake (Townsend 1956),

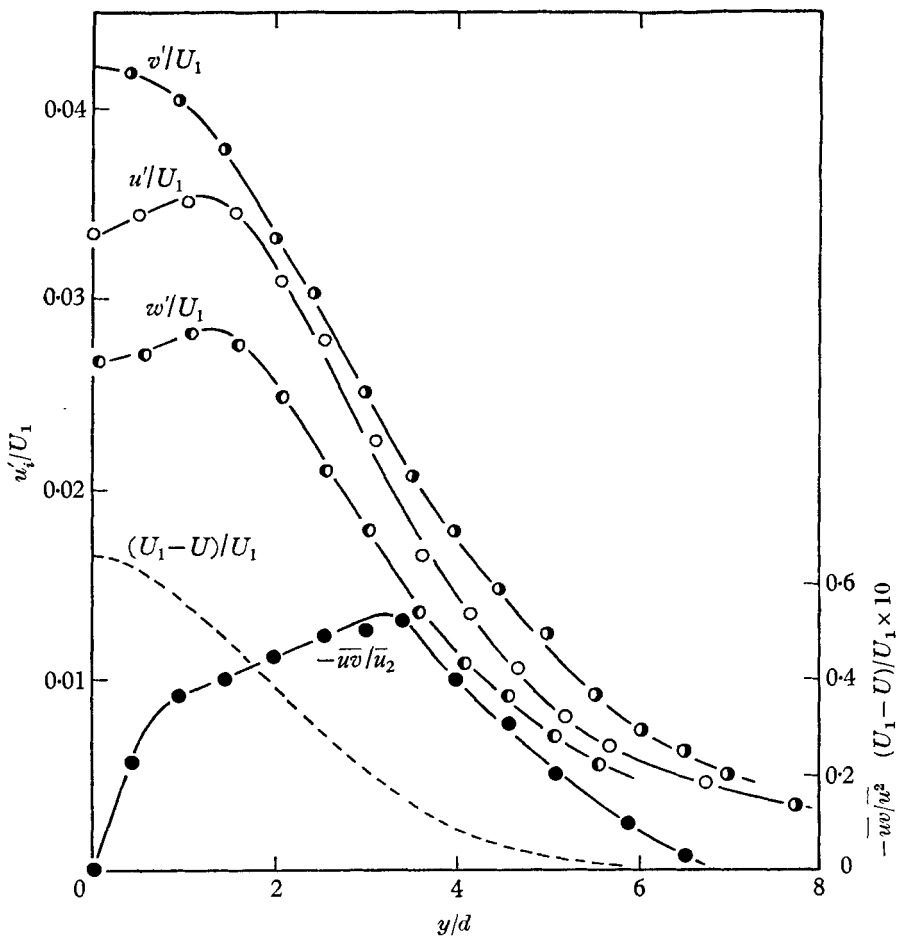

FIGURE 5. Lateral variation of turbulent intensities. (x_0-x_c) = 10 in., $(x-x_c)/d$ = 210, d = $\frac{3}{16}$ in., Re_d = 1700.

remaining roughly constant over the mid-section of the half wake. The peak value of 0·54 is higher, however. This can be explained by examining the way in which the strain influences the structure of the Reynolds-stress term.

The principal axes of the strain field produced by the shear in a wake flow are approximately 45° to the x- and y-directions, and it is possible to define intensity components along these axes:

$$u_s = (u-v)/\sqrt{2}, \tag{3.1}$$

$$v_s = (u+v)/\sqrt{2}. \tag{3.2}$$

The general effect of applying an external strain to the wake, of the form

described by (2.6), would be to increase the magnitude of v relative to u, thus increasing v_s while decreasing u_s compared to unstrained-wake data, and, since

$$-\overline{uv} = \tfrac{1}{2}(\overline{u_s^2} - \overline{v_s^2}), \tag{3.3}$$

the value of the Reynolds stress at identical $(x-x_c)/d$ would be smaller in the presence of the applied strain field. Figure 6 shows that in regions for which $y/d > 2$, and where the effect of the external strain is predominant, the Reynolds

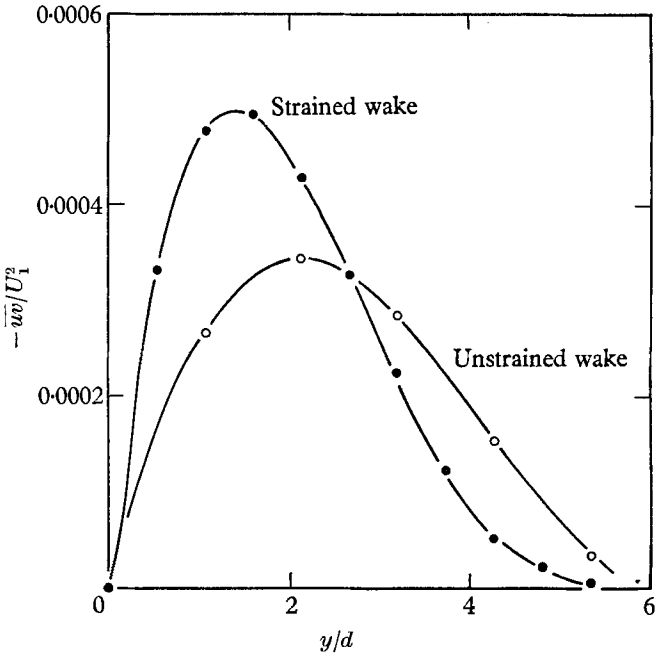

FIGURE 6. Lateral variation of Reynolds stress. $(x-x_c)/d = 210$.

stress is significantly less than for the unstrained wake. If we assume that eddies in this region of the flow have their circulation in planes y = const. and axes aligned $\pm 45°$ to Ox, as the turbulent-velocity correlations of Grant (1958) appear to suggest, then a compression of these eddies in the y-direction, as dictated by the external strain, will attenuate strongly the u-component of the turbulent intensity. The value of the stress coefficient $-\overline{uv}/\overline{u^2}$ would thus be relatively higher than in the normal wake, which is consistent with the present results.

4. Structure of the wake

4.1. *General characteristics*

An examination of the lateral length scales for the $\frac{3}{16}$ in. cylinder in figures 2 and 3 shows that, in the early stages of the straining motion, the mean wake width appears to undergo a rapid expansion before settling into the equilibrium state. This occurs irrespective of the point at which the strain is applied to the wake. To investigate the structure of the wake during this critical period of develop-

ment, a flow visualization technique was devised. Titanium-tetrachloride ($TiCl_4$) which produces a dense white smoke upon contact with air, was applied to the rear of the cylinder. The smoke diffused rapidly into wake, thus delineating the turbulent fluid, and was photographed using an electronic flash to stop the motion, as well as a ciné camera to follow the development of the motion. Figure 7, plate 1, shows the resulting structure of the wake over the first half of the duct. The Reynolds number of 350 is well above the critical point at which the Kármán vortex breaks up into fully turbulent flow. At higher stream velocities the smoke became too diffuse for satisfactory observation, and for Reynolds numbers in the range of 1700, at which the length and velocity scales were determined, oscillograph records were made of hot-wire traces, and the structure of the wake interpreted from these measurements.

The photographic and oscillographic records indicate a predominantly strong motion of the large eddies. Lateral outward-moving jets of turbulent fluid are released from within the wake in the early stages of the flow, and are forced back by the convecting field towards the wake centre. Localized pockets of fluid having vorticity predominantly in the y-direction are thus formed, which are then correctly orientated to receive energy from the strain. The size and intensity of the motion become more pronounced as the total strain increases. There is a general resemblance to the 'jets' described by Grant (1958) for the unstrained wake, but in the present case the eddies appear to be more regular and intense. A well-defined periodicity is evident. The eddies tend to travel in clusters of 3 or 4 with a frequency, observed from oscillograph records and ciné photographs, which varies from group to group, and is approximately $\frac{1}{3}$ to $\frac{1}{4}$ that of the Kármán street. Figure 7 (plate 1) shows an eddy spacing s/d of approximately 15, which at that velocity represents a frequency of 14·7 c/s. The corresponding Kármán street frequency at $\mathrm{Re}_d = 350$ is 42 c/s giving a frequency ratio of 0·36.

There is no observable correlation between eddies on alternate sides of the wake, since they may be alternately spaced or arranged symmetrically. This behaviour is plausible in an equilibrium flow, only if on the average there are as many eddies on one side of the wake as the other. A lack of balance in the large motions would result in an asymmetrical pressure distribution across the wake which might eventually generate a new series of 'jets' on the opposite side. One would then expect to find these motions absolutely correlated to those on the other side. The evidence, however, does not appear to support this possibility, and the suggestion is, that the large motions on one side of the wake are formed independently from those on the other side. This occurs early in the development of the turbulence. Figure 7 shows clearly the variation in the spacing.

Using two hot wires separated in the x-direction, the gross longitudinal convection velocity of the large eddies was measured. They were found to travel at a speed slightly greater than their position within the mean-velocity-defect zone would indicate. One may thus visualize the motion as a system of discrete eddies, carrying little horizontal momentum, the outer being sheared by the external stream and dragged along with it.

The selective amplification of the large motions can be examined from measurements of the distribution of kinetic energy over the spectral range of the tur-

bulence. To illustrate the effect of the external strain more clearly, the variation of the longitudinal one-dimensional spectrum, defined by

$$\overline{u_1^2} = \int_0^\infty E_1(n)\,dn, \tag{4.1.1}$$

is shown first (figure 8) for the undistorted wake, as a function of the downstream distance from the cylinder $(x-x_c)/d$. The values are plotted in terms of wave number

$$k = 2\pi n/U_1, \tag{4.1.2}$$

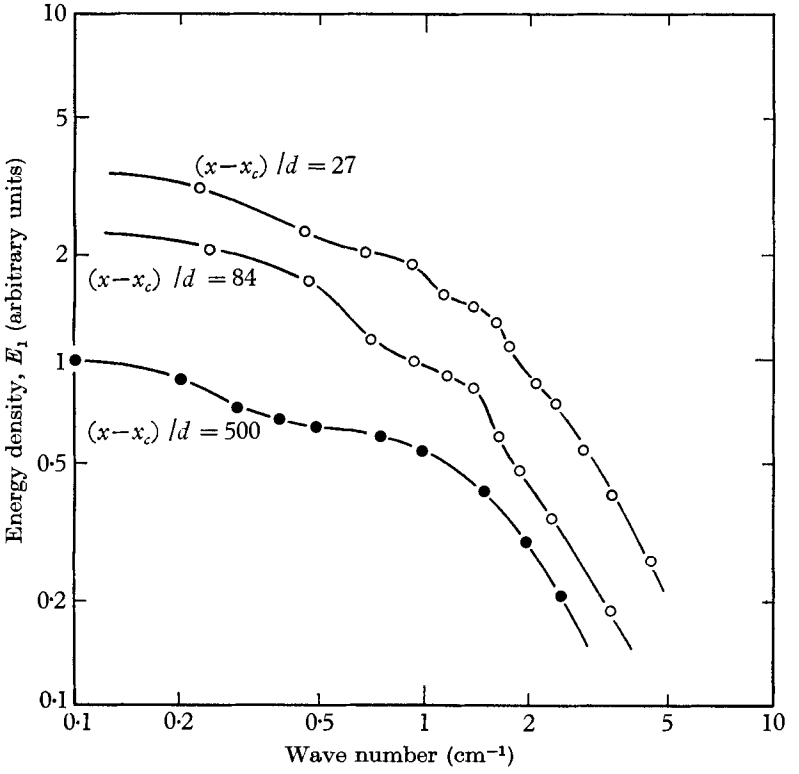

FIGURE 8. Turbulent-energy spectra of the unstrained wake. ●, Re_d = 1300 (Townsend 1950); ○, Re_d = 1700 (Keffer).

so that the results of Townsend (1950) for large $(x-x_c)/d$, and which were made at a different cylinder Reynolds number, could be conveniently included. It can be seen that the characteristic double structure of the wake, which is indicated by the mid-range bumps in the spectrum, persists even up to $(x-x_c)/d = 500$.

The effect of the applied rate of strain upon the structure of the turbulence is indicated by figures 9 and 10. The data are presented in normalized form, $E_1/\overline{u_1^2}$, to illustrate more precisely the relative change of the distribution in the region of maximum energy content. The shape of the spectrum after the initiation of the external strain changes markedly. The major portion of the turbulent energy is confined to the low frequencies. The intermediate double structure, which persists in the unstrained wake, is almost completely eliminated and the rate of

viscous dissipation is accelerated. No well-defined peak at the low end of the spectrum is observed, however. This probably results from a number of effects. The large motions are generally diffuse and their frequency varies over rather wide limits. A sharp local peak in the u-spectrum, such as is observed with the Kármán street, would occur only for an extremely regular and undiffused system of vortices. Also the present spectrum measurements, which were taken in the wake centre, tended to receive contributions from both sides of the wake, and a smearing of the spectrum results.

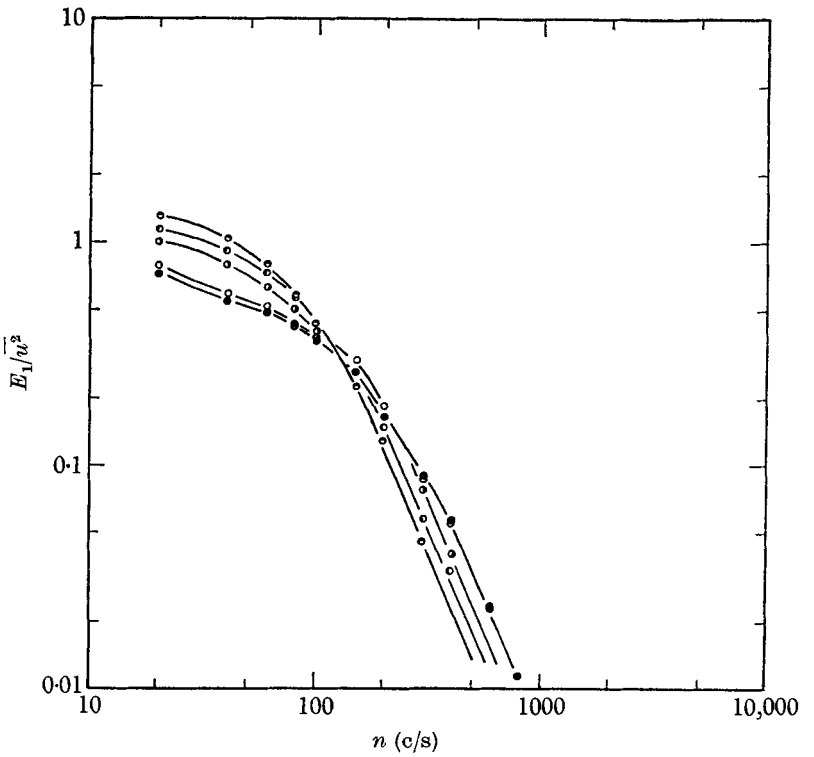

FIGURE 9. Effect of the rate of strain upon the turbulent-energy spectra of the wake. $(x_0-x_c) = 10$ in., $Re_d = 1700$, $d = \frac{3}{16}$ in.; ◓, $(x-x_0) = -5$ in.; ◐, $(x-x_0) = 0$; ◑, $(x-x_0) = 5$ in.; ○, $(x-x_0) = 10$ in.; ●, $(x-x_0) = 20$.

Generally then, the experimental results appear to indicate that the distortion acts selectively upon the wake-flow increasing the viscous dissipation and selectively amplifying the large motions which have favourably aligned vorticity. The result is a shift of the energy-containing eddies to the low-wave-number region of the spectrum.

4.2. *The large eddies*

The conditions for the development of the large-eddy structure in the distortion can be examined by considering a simple turbulent line vortex, with axis in the z-direction, moving with the flow at the free-stream velocity U_1. It decays through viscous action and simultaneously gains vorticity from the stretching action of the strain.

The velocity distribution q, for the unstrained eddy is

$$\frac{\partial^2 q}{\partial r^2}+\frac{1}{r}\frac{\partial q}{\partial r}-\frac{q}{r^2}=\frac{1}{\nu_t}\frac{\partial q}{\partial t}, \tag{4.2.1}$$

where ν_t can be considered an effective 'eddy viscosity' of the turbulent fluid. Using a substitution of Taylor (1918)

$$q=\frac{\partial \theta}{\partial r},$$

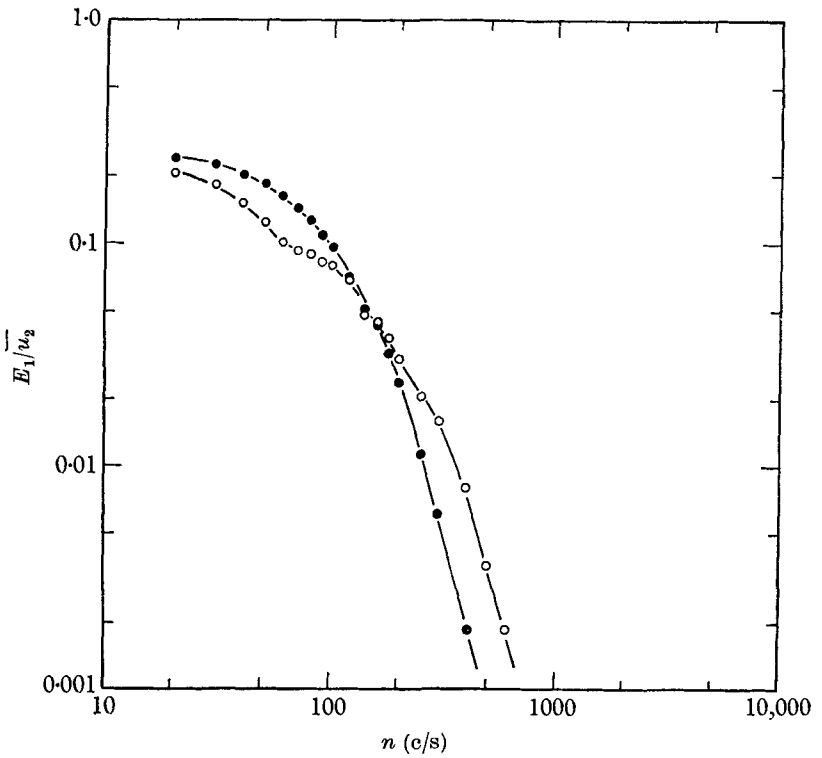

FIGURE 10. Effect of the rate of strain upon the turbulent-energy spectra of the wake. (x_0-x_c) = 20 in., Re_d = 1700, d = $\frac{3}{16}$ in.; ○, $(x-x_0)=-5$ in.; ●, $(x-x_0)$ = 30 in.

the equation of heat conduction is obtained

$$\frac{\partial^2 \theta}{\partial r^2}+\frac{1}{r}\frac{\partial \theta}{\partial r}=\frac{1}{\nu_t}\frac{\partial \theta}{\partial t},$$

with the solution $$\theta = At^{-1}\exp(-r^2/4\nu_t t),$$

which in terms of the velocity field is

$$q=-\frac{Ar}{2\nu_t t^2}\exp(-r^2/4\nu_t t), \tag{4.2.2}$$

where A is a constant which can be determined from the initial conditions of the eddy.

The distribution of velocity has a maximum at the point

$$r_m = \sqrt{(2\nu_t t)}, \tag{4.2.3}$$

and it is convenient to define the size of the eddy in terms of this radius. t represents a fictitious time for the growth and decay of the turbulent eddy.

Following the motion of the eddy through the distortion, the change in vorticity ζ resulting from the application of a pure strain rate will be

$$\frac{D\zeta}{Dt} = \alpha_{33}\zeta,$$

which can be solved directly for the vorticity distribution across the eddy, giving

$$\zeta = \zeta_0 \exp\left(\int_{t_0}^{t} \alpha_{33}\, dt\right).$$

For the present flow $\alpha_{33} = aU_1$, so that

$$\zeta = \zeta_0 \exp\{aU_1(t-t_0)\} \quad \text{with} \quad t > t_0,$$

where the subscript zero refers to conditions just prior to the application of the strain. The strain rate thus acts directly upon each circulation path, and so the change in the velocity distribution within the eddy when independently strained by the distortion and decaying through turbulent viscous processes is

$$q = -\frac{Ar}{2\nu_t t^2} \exp\{-(r^2/4\nu_t t) + aU_1(t-t_0)\} \quad (t > t_0). \tag{4.2.4}$$

To extend this analysis to the present situation, it is necessary to specify the characteristics of the eddy just as it enters the distortion field. An approximate indication of the eddy size can be obtained by an inspection of oscillograph traces, by defining, as in (4.2.3), the interval between the positive and negative peaks in the velocity distribution of the eddy as $2r_m$. This procedure was complicated by the presence of a fine-scale-turbulence structure superimposed upon the signal, but the estimation of r_m is certain to be at least of the right order of magnitude. For the $\frac{3}{16}$ in. diameter cylinder positioned 10 in. upstream from the distortion and $Re_d = 1700$, the average eddy radius immediately before entering the strain field, i.e. $t = t_0$, was

$$(r_m)_0/d \approx 2{\cdot}85,$$

or

$$(r_m)_0 \approx 0{\cdot}0445 \text{ ft.}$$

The coefficient of turbulent viscosity within the eddy will be of the same order as the 'virtual eddy viscosity' defined by

$$\bar{\nu}_t = -\overline{uv}/(\partial U/\partial y) \tag{4.2.5}$$

averaged over the wake. For this flow $\bar{\nu}_t$ was approximately 0·0055 ft.^{2}/sec. With this value, the time which specifies the fictitious development of the eddy up to the entrance of the distortion is obtained from (4.2.3)

$$t_0 = (r_m)_0^2/2\bar{\nu}_t = 0{\cdot}18 \text{ sec.}$$

The change in the velocity distribution of the eddy as it moves through the strain field can now be calculated from (4.2.4) and the results are plotted dimensionlessly as a function of the total-strain ratio β in figure 11.

During the application of the strain, the eddy size, equation (4.2.3), increases slowly. The intensity of the eddy is characterized by the maximum velocity

$$q_m = -A'\nu_t^{-\frac{1}{2}}t^{-\frac{3}{2}}\exp\{aU_1(t-t_0)\}, \tag{4.2.6}$$

and it increases moderately up to strain ratios of $\beta = 2{\cdot}5$. Past this point, the increase is more marked as the exponential term in equation (4.2.6) dominates. The dashed line shows the velocity distribution of a decaying eddy without the presence of the stretching action at the equivalent position $\beta = 4$, i.e. $(x-x_0) = 40$ in.

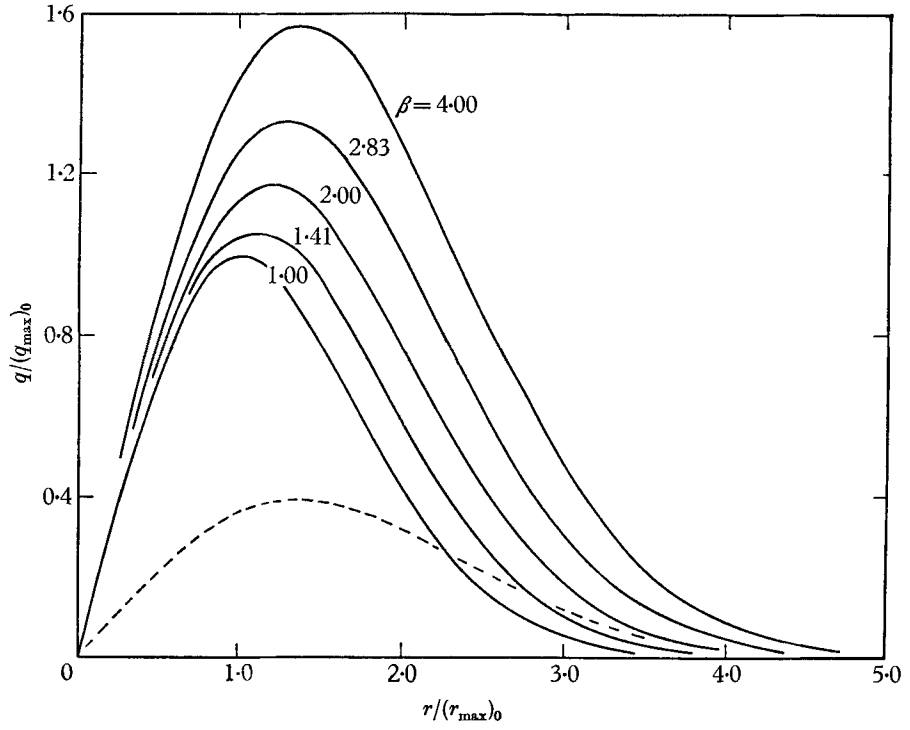

FIGURE 11. Velocity distribution of the model eddy under the influence of strain. – – –, Unstrained eddy at $(x-x_0) = 40$ in.

The very much simplified model described above agrees qualitatively with observations of the flow. Ciné pictures show clearly a gradual increase in the intensity and size of the eddy motions up to values of about $\beta = 2{\cdot}5$. At this point the wake appears to be composed solely of these large motions, the intermediate structure being almost completely eliminated. Observations further downstream were difficult as the smoke became too diffuse.

4.3. *The dissipation of turbulent energy*

It is clear from the previous analysis that a system of eddies, correctly orientated to the principal axes of the strain, may increase their total energy content. Similarly, eddies aligned in the other lateral direction would be expected to lose energy more rapidly. However, the smallest eddies of the flow, wherein most of

the viscous dissipation of turbulent motion into thermal energy occurs, are distributed randomly throughout the flow, and it is not immediately obvious that the presence of a strain field, additional to that generated by the wake, should result in a net increase in the rate of dissipation as found by the spectra measurements. It is possible, though, to predict this effect quantitatively and the theory outlined below is shown to be valid for total strains that are not too great.

The complete viscous term in the turbulent energy equation is

$$\overline{\nu u_i \frac{\partial^2 u_i}{\partial x_j^2}} = \nu \frac{\partial^2}{\partial x_j^2}(\tfrac{1}{2}\overline{q}^2) - \nu \overline{\left(\frac{\partial u_i}{\partial x_j}\right)^2}. \tag{4.3.1}$$

For most shear flows the viscous diffusion may be neglected so that the right-hand quantity only, need be considered. In a homogeneous isotropic flow this reduces simply to

$$\epsilon = 15\nu\overline{(\partial u/\partial x)^2}. \tag{4.3.2}$$

In order to obtain an equivalent relationship for the strained flow, two assumptions are necessary:

(1) The dissipating eddies prior to their entry into the distortion are in a state of local isotropy, a condition which has been demonstrated by Townsend to be sufficiently accurate for most purposes.

(2) The wake is strained homogeneously and rapidly enough so that we need first of all consider only a geometric distortion of the structure.

The latter condition is potentially very restrictive. However, a real fluid requires a finite reaction time to adjust its structure to the strain, and it is reasonable to expect that second-order effects would not become significantly important, at least for small total strains.

The constant-rate-of-strain field affects the various dissipation terms then directly as their orientation to the principal axes of the strain. The result is that the local spatial gradients will change upon entering the distortion as

$$\left.\begin{aligned} \left(\frac{\partial}{\partial x}\right) &= \left(\frac{\partial}{\partial x}\right)_0, \\ \left(\frac{\partial}{\partial y}\right) &= \frac{1}{\beta}\left(\frac{\partial}{\partial y}\right)_0, \\ \left(\frac{\partial}{\partial z}\right) &= \frac{1}{\beta^{-1}}\left(\frac{\partial}{\partial z}\right)_0. \end{aligned}\right\} \tag{4.3.3}$$

The subscript refers to the appropriate unstrained value at the particular point in question, that is the isotropic equivalent. Applying these relations to the individual terms in the dissipation expression, and ignoring, for the moment, the first-order changes in intensity of the components, we have simply

$$\epsilon_d = 5\nu(1+\beta^{-2}+\beta^2)\overline{\left(\frac{\partial u}{\partial x}\right)_0^2}, \tag{4.3.4}$$

and comparing this to the isotropic value we obtain the ratio

$$\epsilon_d/\epsilon_0 = \tfrac{1}{3}(1+\beta^{-2}+\beta^2). \tag{4.3.5}$$

The requirement for an increase in the dissipation rate is simply that $\beta > 1$. For $\beta = 1$, the expression reduces to the isotropic condition.

The effect of including the first-order changes in intensity can be examined directly if equation (4.3.1) is expressed in the form

$$\epsilon = \nu \overline{\left(\frac{\partial u_i}{\partial x_j}\right)^2} = \nu \frac{\overline{u_i^2}}{\lambda_j^2}, \tag{4.3.6}$$

where λ_j is a length scale associated with the smallest eddies in the flow. Townsend's results for the uniform straining of a homogeneous turbulence allow the first-order changes in the components to be written as

$$\overline{u^2}/\overline{u_0^2} = 1,$$
$$\overline{v^2}/\overline{v_0^2} = (1+\tfrac{4}{5}k),$$
$$\overline{w^2}/\overline{w_0^2} = (1-\tfrac{4}{5}k),$$

where
$$k = (\beta-\beta^{-1})/(\beta+\beta^{-1}),$$

and, assuming that the length scales distort geometrically with the applied strain as we did for the local spatial gradients, equation (4.3.6) leads to expressions of the type

$$\overline{\left(\frac{\partial v}{\partial y}\right)^2} = \frac{\overline{v^2}}{\lambda_v^2} = \frac{1+\frac{4}{5}k}{\beta^2}\left(\frac{\overline{v^2}}{\lambda_v^2}\right)_0 = \frac{1+\frac{4}{5}k}{\beta^2}\left(\frac{\overline{u^2}}{\lambda_u^2}\right)_0.$$

Collecting the various terms and simplifying, we obtain finally

$$\epsilon_d = 5\nu(1+\beta^{-2}+\beta^2)\left(\frac{\overline{u^2}}{\lambda_u^2}\right)_0, \tag{4.3.7}$$

which is structurally identical to (4.3.4). To a first approximation then, the effect of the inertial energy transfer between components can be neglected, and the redistribution of energy would be expected to become significant only as the non-linear terms become important, i.e. as the total amount of energy in the components changes.

To test the range of validity of the theory, a comparison was made with the data of Townsend (1954) for the uniform distortion of homogeneous turbulence. The results are plotted in figure 12. For total strains up to $\beta = 2$, the theory is reasonably successful. For $\beta > 2$, the viscous and inertial transfer terms become significant.

4.4. *Turbulent energy balance*

The balance of turbulent energy across the wake at the plane of symmetry $z = 0$ was given by equation (2.20), which is in dimensionless form

$$\underset{(1)}{\frac{(x-x_c)}{U_1^3}U\frac{\partial(\frac{1}{2}\overline{q^2})}{\partial x}} - \underset{(2)}{\frac{ay(x-x_c)}{U_1^3}U\frac{\partial(\frac{1}{2}\overline{q^2})}{\partial y}} + \underset{(3)}{\frac{(x-x_c)}{U_1^3}\overline{uv}\frac{\partial U}{\partial y}} - \underset{(4)}{\frac{(x-x_c)}{U_1^3}(\overline{v^2}-\overline{w^2})aU}$$
$$+ \underset{(5)}{\frac{(x-x_c)}{U_1^3}\frac{\partial}{\partial y}\overline{v\left(\frac{p}{\rho}+\frac{q^2}{2}\right)}} + \underset{(6)}{\frac{(x-x_c)}{U_1^3}\epsilon} = 0. \tag{4.4.1}$$

The lateral diffusion of energy by turbulent motions, term (5), is of particular significance in the description of the large eddy motions. Unfortunately, it is not

directly measurable by present techniques and must be inferred by difference from the other terms in the balance. Figure 13 shows the distribution of energy across the distorted wake at the position $(x-x_c)/d = 210$ for the strain applied at $(x_0-x_c)/d = 105$. A discussion of the terms follows and comparisons are drawn to the data of Townsend (1956) for the unstrained wake which were taken at a position closer to the cylinder, $(x-x_c)/d = 160$.

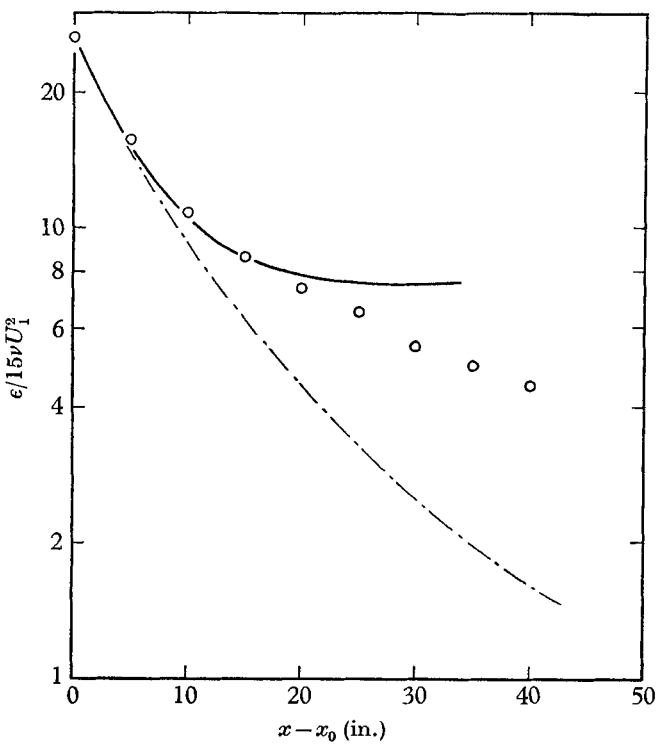

FIGURE 12. Effect of distortion on the dissipation of homogeneous turbulence. ○, Townsend (1954); ——, rapid-strain theory; — - —, unstrained homogeneous turbulence.

The advection of turbulent energy by the mean flow is described by the first two terms in (4.4.1). The longitudinal convection term is similar to the unstrained wake, with the exception that the loss of turbulent energy in the outer half of the wake is considerably smaller. This is not unreasonable. The distortion constrains the flow in the (x, y)-plane, and the probability of traversing through a region having a positive energy gradient in the x-direction (which in the unstrained wake arises from a lateral divergence of the mean-flow streamlines) is appreciably less. The second advection term is interesting. Over most of the wake it is positive, denoting an inward flow of kinetic energy to the wake centre as the direction of the lateral convective flow would suggest. Just at the wake centre, however, a small negative region occurs due to the local change of sign of the y-energy gradient. In the present case, the change in the gradient is more marked than in the unstrained wake.

The production of turbulent energy by the Reynolds stress working against the mean velocity gradient, term (3), is similar in form but greater in magnitude than

that in the unstrained wake since $-\overline{uv}/U_1^2$ is larger (figure 6). The energy production which arises from the effect of the strain rate, term (4), is of the expected form, having a maximum at the wake centre where the anisotropy of the intensities is most pronounced (figure 5).

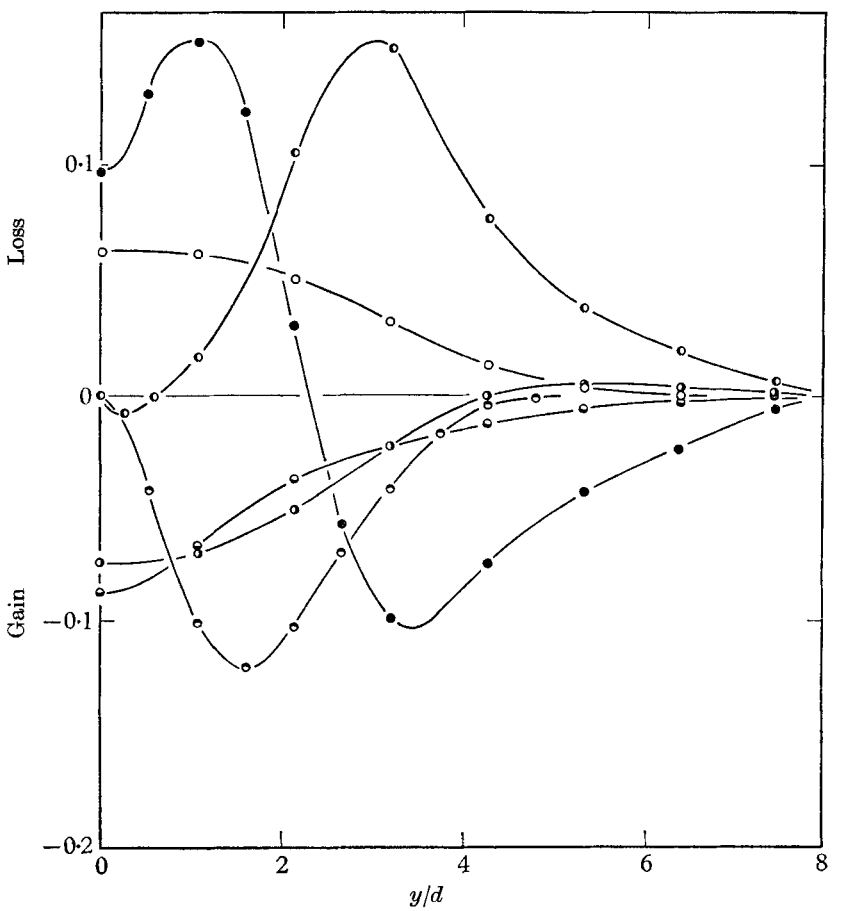

FIGURE 13. Turbulent-energy balance. $(x-x_c)/d = 210$, $Re_d = 1700$, $d = \frac{3}{16}$ in., $(x-x_0) = 30$ in.; ◑, longitudinal advection (1); ◐, lateral advection (2); ◓, shear production (3); ◒, distortion production (4); ●, lateral diffusion (5); ○, dissipation (6).

The longitudinal component of the dissipation term was calculated from the turbulent intensity and measurements of the small eddy scale λ^2, determined by a count of the zero crossings of the turbulent signal on oscillograph traces. Using the strained-isotropic-turbulence relation (4.3.8), the full dissipation term was evaluated. The functional shape of ϵ is similar to the unstrained wake, which is not surprising since the strain is applied uniformly.

The lateral diffusion term (5) which has been determined by difference, includes two physically distinct but not separable processes: the flow of energy down the pressure gradient and the movement of kinetic energy by turbulent diffusion. They have been shown to be of the same order in the unstrained wake,

and it can be assumed that this will be so in the present case. The contribution of this term to the energy balance is proportionately greater than in the unstrained wake, which can be considered evidence of the greater activity of the lateral motions. In general shape, the function is identical to the unstrained wake, which is reasonable since the mechanisms operating in the two cases cannot be very different. A rather important check, which tends to substantiate the accuracy of the other quantities in the energy balance, is that the diffusion term integrates to zero across the wake width, within 2 %.

The exact means by which the turbulent energy is diffused laterally across the wake is not clear, and must be inferred from an analysis of the results. A gradient type of diffusion is certain to exist. This not likely to be a complete description of the process, however, since the effective diffusion coefficient which is determined from this approach has no functional similarity to the calculated value of the virtual eddy viscosity, which can be obtained by more direct methods. It has been generally recognized that in the unstrained wake a lateral bulk-convection motion plays a significant part in the turbulent diffusion (Townsend 1956). Assuming both of the above mechanisms to be important, we can, in the present case, consider that they act independently and define an effective bulk convection velocity $\mathscr{V}$ from the expression

$$\overline{v\left(\frac{p}{\rho}+\frac{q^2}{2}\right)} = -\kappa\frac{\partial(\frac{1}{2}\overline{q^2})}{\partial y}+\mathscr{V}\frac{\overline{q^2}}{2}, \tag{4.4.2}$$

where κ is a virtual eddy viscosity for the turbulent energy. For a gradient type diffusion, simple mixing-length theory implies that momentum- and energy-diffusion coefficients are directly proportional to the mean-velocity-defect and turbulent-velocity scales, l_0 and l_0' respectively, so that κ can be evaluated by specifying a Schmidt number

$$\kappa = \nu_t\left(\frac{l_0'}{l_0}\right)^2 = \frac{-\overline{uv}}{\partial U/\partial y}\left(\frac{l_0'}{l_0}\right)^2.$$

The rest of the terms in (4.4.2) are determined from the experimental data, thereby establishing $\mathscr{V}$.

Figure 14 shows the resulting variation of $\mathscr{V}/U_1$ across the wake, and for comparison unstrained-wake data of Townsend (1956) at $(x-x_0)/d = 160$. The latter values represent the contribution to the bulk motions arising from the triple correlation term, $\partial(\frac{1}{2}\overline{vq^2})/\partial y$ only, which was measured directly. As well, the effect of the gradient diffusion was not eliminated, and thus a quantitative comparison with the distorted wake over the whole width of the wake is not possible. In the outer regions, however, where gradient diffusion is negligible, the differences in the form of the distributions can be assessed reasonably well. The bulk motion in the strained wake appears to be closely confined to the outer wake and is marked by a more rapid increase in magnitude in the mid-wake and a sharper deceleration at the edge. The latter effect is undoubtedly caused by the inward convection of the main stream ayU/U_1, which at the wake edge is of the same order as the maximum value of $\mathscr{V}/U_1$. Figure 7 shows the restrictions of the lateral motions clearly.

The reason for the presence of the rapid acceleration in $\mathscr{V}/U_1$ is not immediately obvious. The maximum value of Reynolds stress in the strained wake (figure 6) is high relative to the undistorted wake. This effective anisotropy (equations (3.1) and (3.2)) cannot persist up to very large values of y/d in the presence of the applied strain field, and the large bulk motions may, as suggested by Grant, be

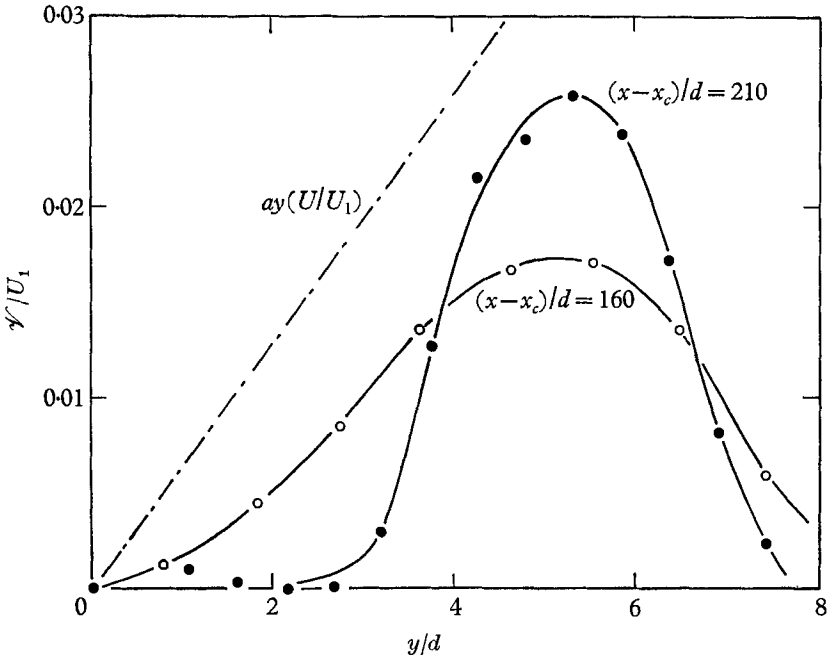

FIGURE 14. Bulk convection velocity. ○, Townsend (1956); ●, Keffer.

the manifestation of a stress-relief process by secondary flows. This notion is not inconsistent with the present results. The region of the wake in which the Reynolds stress decreases coincides reasonably well with the acceleration point of the lateral bulk motions. One could explain the observed intensity of the bulk convection in the present case then as simply a result of the relatively high value of $-\overline{uv}/U_1^2$.

5. Conclusion

From the above analyses it is possible to assess the significance of the large-eddy motions in the flow system. Prior to the application of the strain, the turbulent wake develops large 'jet-type', lateral motions of the form observed by Grant (1958), which can be considered as the normal mechanism for relieving the interior stresses in the flow. Upon entering the distorting section of the tunnel, a rapid widening of the wake occurs, as a consequence of the more active secondary motions required to release the relatively larger $-\overline{uv}$ stresses which have been set up. As the total strain increases, the inward lateral convection of the mean flow, in the y-direction, restricts the path of the 'jets', forcing them to curl back towards the wake centre. This creates a favourably orientated region of

circulation upon which the rate of strain can act, with the result that the large motions are selectively amplified producing a quasi-periodic system of large eddies. The motion can be compared qualitatively to a group of turbulent line vortices with axes in the z-direction, convected by the mean flow, gaining vorticity from the lateral strain rate and simultaneously losing energy through turbulent viscous decay. In the present case the strain rate is large enough so that there is a net increase in the vortex strength. The competitive processes of vortex stretching and lateral diffusion of the velocity field within each eddy appear to stabilize the turbulent motion, preventing any further random outbursts of the turbulent front, which would be expected of a normally developing turbulent shear flow.

Attendant upon the selective amplification of the large eddies is an increased activity of the large-wave-number components. The smallest eddies of the flow, which have a random orientation to the principal axes of strain, are stretched and contorted by the strain, thus hastening the process of viscous dissipation. The main bulk of the turbulent kinetic energy, therefore, becomes localized within the large eddies, effecting a shift in the energy spectrum to low wave-numbers. The result is that, for total strains of the order $\beta = 2$, the large eddies completely dominate the flow, eventually to such an extent that gaps appear in the turbulent structure of the wake, in some cases extending even to the centre of the flow.

The presence of the large eddies appears to prevent a complete approach to the theoretically predicted self-preservation state. Conditions suitable for self-preservation require a coupling of the turbulence structure to the mean momentum terms via the Navier–Stokes equations. In the present case, the influence of the rate of strain upon the eddies predominates, and it is these non-randomly orientated eddies which control the development.

It is of considerable interest to examine the question of the origin of the large-eddy motion. Townsend suggests that, in simple wake flows, chance configurations of circulation occur within the turbulent field, which, if favourably situated, gain energy from the rate-of-strain field produced by the mean-velocity defect of the wake. Such an eddy goes through a growth phase, aligning itself more closely to the strain axis, and finally reaching an equilibrium state. It is difficult to see just how the observed quasi-periodicity could develop from this model, however.

One possibility is that the motions have their origin in the line vortex which is formed immediately behind the cylinder before the break-up into turbulence takes place. Wake-flow measurements generally have revealed a spanwise variation in the velocity distribution at this point, similar to that found by Hama, Long & Hegarty (1957) in the boundary layer. In the present case, this transverse wave structure was evidenced by a lateral contorting of the line vortex, producing a 'horse-shoe' shaped structure. Such a configuration would be sheared in the plane of the cylinder by the mean stream, thus generating a local region having circulation of the same sign as the Kármán street but larger and much more diffuse. The frequency of such motions would have no direct relationship to the Kármán frequency, which is consistent with the present observations, but would depend upon the position of the lateral contortions of the line vortex and the

frequency with which the motions develop. Once formed, these motions would be the most likely source wherein the stress-relief mechanism, mentioned above, could occur.

This explanation receives some support from oscillograph traces of the velocity variation immediately behind the cylinder, before fully developed turbulence sets in. Observations show a periodic modulation of the sinusoidal pattern. The frequency of the modulations was of the order of the large-eddy motions, which could be taken as evidence of a shedding frequency of the contorted line vortex. The modulations are identical to the effect noticed upon the Tollmien–Schlichting waves in a boundary layer, and it is evident that much the same mechanism is acting in the wake.

The author would like to thank Dr A. A. Townsend for the opportunity of working in his laboratory and with whom he had many interesting discussions on this problem. Throughout the period of work, the author was in receipt of a post-doctoral fellowship from the National Research Council of Canada and for which he expresses thanks.

REFERENCES

BATCHELOR, G. K. & PROUDMAN, I. 1954 *Quart. J. Mech. Appl. Math.* **7**, 83.

GRANT, H. L. 1958 *J. Fluid Mech.* **4**, 149.

HAMA, F. R., LONG, J. D. & HEGARTY, J. C. 1957 *J. Appl. Phys.* **28**, 388.

PRANDTL, L. 1933 *NACA TM* no. 726.

REYNOLDS, A. J. 1962 *J. Fluid Mech.* **13**, 333.

RIBNER, H. S. & TUCKER, M. 1952 *NACA TN* no. 2606.

TAYLOR, G. I. 1918 *ARC R & M* no. 598.

TAYLOR, G. I. 1935 *Z. angew. Math. Mech.* **15**, 91.

TOWNSEND, A. A. 1950 *Phil. Mag.* **41**, 890.

TOWNSEND, A. A. 1954 *Quart. J. Mech. Appl. Math.* **7**, 104.

TOWNSEND, A. A. 1956 *The Structure of Turbulent Shear Flow.* Cambridge University Press.